LIGHTWEIGHT COMPOSITE PRESSURE HOUSINGS FOR MID-WATER AND BENTHIC APPLICATIONS

V. Papazoglou[1], F. Livingstone[2], P. Chauchot[3], G. Jennequin[4], I. Kilpatrick[2], R. Meddes[5], P. Stevenson[6], V. Antonelli[7], N. Tsouvalis[1] and J. Williams[8]

[1]School of Naval Architecture and Marine Engineering, National Technical University of Athens, Greece
[2]QinetiQ Ltd, Rosyth, UK
[3]Institut Français de Recherche pour l' Exploitation de la Mer, IFREMER, Brest, France
[4]Constructions Industrielles de la Méditerranée, CNIM, France
[5]QinetiQ Ltd, Farnborough, UK
[6]Southampton Oceanography Centre, UK
[7]Centre of Lightweight Structures TUD-TNO, The Netherlands
[8]Marinetech South Ltd, MTS, UK

ABSTRACT

This paper outlines the work undertaken within the project *Lightweight composite pressure housings for mid-water and benthic applications*, leading to the successful testing of a large all composite AUV pressure housing, to the equivalent of 2,000-metre sea depth with a factor of safety exceeding 1.5. It briefly deals with the preliminary operational requirements and material selection, the initial design, modelling, fabrication and subsequent testing of small scale, filament wound, CFRP test cylinders and of large scale, resin transfer moulded, CFRP end-domes, the design of metallic transition rings, and the design of a large, 450mm internal diameter, filament wound CFRP AUV pressure hull cylinder closed by Titanium end-domes. This, along with large composite end-domes and a number of small scale test cylinders were subjected to a long-term creep test in the working environment. The paper describes also the design, modelling, fabrication and testing of the large, 450 mm internal diameter, all composite AUV demonstrator pressure hull.

1. INTRODUCTION

The continuing and growing need for observational data in support of climate research, pollution monitoring, oceanographic and archaeological survey, and commercial deep ocean or sea bed exploration has stimulated interest in the use of unmanned autonomous underwater vehicles (AUV's) and the long-term deployment of instruments within benthic landers. Free swimming, high payload, long endurance AUV's are an attractive alternative to the more common deep-towed systems, remotely operated vehicles (ROV's), manned submersibles and in some situations stationary moored instruments. The design of benthic landers, which incorporate pressure housings (for instrumentation and power) along with chambers of various sizes for controlled environment monitoring, requires a careful balance between overall weight and buoyancy. Composite materials, and in particular fiber reinforced polymers (FRP), with their high strength to weight ratio and their good weight to buoyancy ratio, are ideally suited for these applications. This paper outlines the research undertaken within the EC partially funded MAST III project, *Lightweight composite pressure housings for mid-water and benthic applications*, MAS3-CT97-0091, culminating in the successful testing of a large all composite AUV pressure housing, to the equivalent of 2,000 m sea depth with a factor of safety exceeding 1.5.

For the purpose of the project it was decided to focus on the pressure hull (450 mm internal diameter) of an AUV with a designed operational capability of 2,000 m. It was felt that 2,000 m provides a realistic near term target which covers the upper ocean, a zone of major scientific attention and commercial exploration. The AUV demonstrator hull consists of a filament wound carbon fibre reinforced polymer (CFRP) cylinder with resin transfer moulded (RTM) carbon fibre end-domes connected via Titanium (Ti-6Al-4V) transition rings.

The relative merits of framed (ring stiffened), monocoque and sandwich cylinders were considered. Monocoque hulls represent a lower risk, are cheaper and easier to fabricate by filament winding, and are more readily analysed theoretically. Frame stiffened hulls may be more efficient in the longer term and can be fabricated by filament winding, but design tools

Table1. AUV and Benthic lander Specifications.

Autonomous Underwater Vehicle		**Benthic Lander**	
Maximum depth	6,000 m	Max. working depth	50 – 7,000 m
Speed	5.5 ± 0.5 knots	Weight in air	200 – 1,800 kg
Range	200 – 1,000 km	Overall weight in water	75 – 150 kg
Mission duration	20 days	Mission duration	4 – 120 days
Mission frequency	5 per year	Bottom deployment	0.5 – 50 days
Life time	10 years	Descent rate	150 – 360 bar/hr
Descent/ascent rate	300 bar/hr	Positive buoyancy	45 – 250 kg
Service time	6 hours	Ascent rate	120 – 360 bar/hr
Dives to max. depth	100 per year		

are not proven. Sandwich hulls may also be an attractive option but, again, design tools are not proven and there is limited experimental data. Consequently it was decided to opt for a monocoque hull design.

Great importance was attached to the modelling, through numerical (finite element) and analytical methods, of the performance of the hull design and to the subsequent comparison with experimental results. A series of small scale, 175 mm internal diameter, cylinders were fabricated and experimentally tested. This was done to assess both the fabrication procedures and modelling tools. In addition, a series of long-term material tests were conducted on small and large scale specimens, moored at sea for twelve months at a depth of 2,000 m.

2. REQUIREMENTS AND MATERIAL SELECTION

The generic specifications considered for a free swimming, high payload, long endurance AUV are shown in Table 1 [1]. An AUV with a 6,000 m operational depth will cover approximately 97% of the world's seabed, the remainder being mostly deep-sea trenches. As explained, though, in the Introduction, the present project limited itself to an operational capability of 2,000 m. At 5 or 6 knots it is as fast as the majority of current ROV's, while the independence from a mother ship/platform has significant cost and operational benefits. The capability to be pre-programmed to surface for the transmission of the collected data and then be re-programmed or continue with the task or to rendezvous at a prearranged location and time provides additional flexibility and operational benefits.

Cylinders and domes were fabricated from TENAX J UTS carbon fibre and appropriate resin systems, with the mechanical properties provided in reference [1].

3. DESIGN AND FABRICATION

3.1 Small scale cylinders

Prior to fabrication and experimental testing, various stacking sequences and thickness (6, 8, 10, 12 and 20 mm) were considered for the small scale test specimens, Fig. 1. Eigenvalue buckling, non-linear buckling and linear stress analysis were performed to establish the maximum buckling pressure [2]. Stacking sequences considered for each thickness were: $(\pm\theta)_n$, $(90°/\pm\theta)_n$ and $[90°_n/(\pm\theta)_n]$, where n is the number of repetitions, while the 90° layer(s) of the last two sequences are on the inside of the cylinder. The values of 'θ' considered were 15°, 30°, 45°, 55°, 60° and 75°. In addition, a fourth optimised stacking sequence (Case 4), which is different for each thickness, was considered, as outlined in Table 2.

The results of this analysis, an example of which is shown in Fig. 2, indicated that the optimised 'Case 4' stacking sequences result in stiffer cylinders than any of the other three

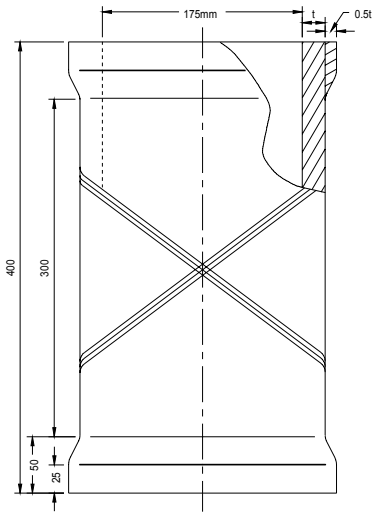

Fig. 1. Small scale test cylinder.

Table 2. Case 4, optimised stacking sequences.

Cylinder thickness	**Stacking sequence**
6 mm thick cylinder	$[(90°)_4/\pm60°/(\pm30°)_5/\pm60°/(90°)_2]$
8 mm thick cylinder	$[(90°)_4/\pm75°/(\pm30°)_8/\pm75°/(90°)_2]$
10 mm thick cylinder	$[(90°)_6/\pm75°/\pm45°/(\pm30°)_8/\pm60°/(90°)_4]$
12 mm thick cylinder	$[(90°)_8/\pm75°/\pm60°/(\pm30°)_9/(90°)_8]$
20 mm thick cylinder	$[(90°)_{16}/(\pm60°)_3/\pm45°/(\pm30°)_3/(90°)_2/(\pm30°)_7/(90°)_2/\pm30°/\pm75°/(90°)_{12}]$

cases. This conclusion stems from both eigenvalue and non-linear analysis [2]. The second best stacking sequence is $[90°_n/(\pm\theta)_n]$, where 'θ' lies between 50° and 60°, depending on thickness.

The design of the flat plate end-closures for the small scale cylinder tests (hydrostatic and creep) was optimised to reduce the stresses at the cylinder/end-closure interface [3]. The optimised design consists of Aluminium alloy end rings bonded to the cylinder ends, to provide simple 'O'-ring sealing, with a thick plate end-closure, which is held in contact with the cylinder ends by external tie-rods and a retaining ring.

3.2 Small cylinder fabrication

Small scale cylinders were fabricated by filament winding. Unfortunately, problems were encountered in the fabrication of the thicker, higher than 8 mm wall thickness, cylinders to the

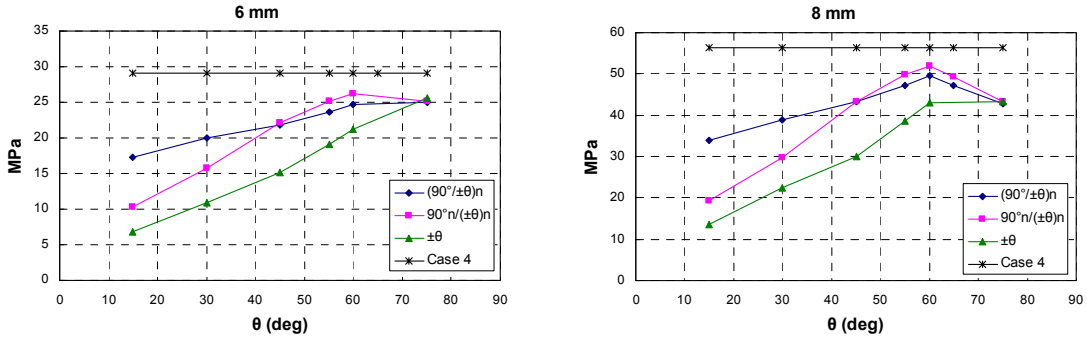

Fig. 2. Buckling load as a function of stacking sequence for t_{cyl}=6 and 8 mm.

optimised winding sequence. Delaminations were detected in the subsequent non-destructive examinations (ultrasonic inspection) and the hydrostatic pressure tests indicated a reduction in buckling strength of about 3 from the theoretical value. This reduction in strength was probably due to poor consolidation and weak interfaces (resin rich) between layers, particularly in the ±30° windings. Cylinders with modified winding sequences and additional 90° layers within the ±30° windings were fabricated in an attempt to overcome the problem. Other options such as, adjusting the winding tension, utilising tape for the final outer cover to consolidate the windings, and multi-step processes (winding and intermediate curing in 2 or 3 phases) were tried and tested. The best compromise was found to be a multi-step winding and curing manufacturing process [4].

3.3 Large scale end-domes

Various conceptual designs of end-domes were considered, analysed and assessed with respect to a number of operational requirements, including fabrication, as summarized in Table 3 [5].

The hybrid design was found to be the most promising shape for this particular application. However, due to fabrication constraints in the RTM process, it is preferable to have a ratio of thickness to radius of curvature of 0.2 to reduce the possibility of delamination and to improve production quality. The hybrid design was therefore slightly modified to form an ellipsoidal shape, which is easier for both production and the subsequent strength and buckling analysis, as it is a simpler shape to define, Fig. 3. A final analysis confirmed that the small change from the hybrid to the ellipsoidal shape had in fact achieved better results, eliminating the large bending effects on the top of the dome. Three sets of domes were fabricated, one set for back-to-back long-term creep tests, one set for back-to-back hydrostatic test and one set for the demonstrator AUV pressure hull.

3.4 Transition ring design

An AUV pressure hull will be expected to carry various oceanographic and scientific payloads that will be periodically removed and re-fitted. Apart from simply sealing the end-domes to the cylindrical body, the end-closure design must allow for the easy removal and installation of payloads, be robust enough to withstand the harsh open conditions found on ships decks, and resistant to dynamic and shock loads from handling, particularly in

Table 3. Summary of end-dome design concepts.

Dome Type	Hemisphere	Glass Hemisphere	Spherical Section	Pressure Vessel Shape	Hybrid
Material	carbon/epoxy	glass/epoxy	carbon/epoxy	carbon/epoxy	carbon/epoxy
Wall thickness (mm)*	30	40/30	40	30/40	30/40
Maximum strain (%)	0.6	0.7	0.4	0.8	0.48
Axial deflection (mm)	0.69	1.71	1.7	3.63	1.73
Buckling (MPa)	36.3	36.3	35.4	53.1	53.1
Height (mm)	225	225	135	142	158
Weight (kg)	16.4	24.2	12.2	12.7	13.0
Ring design	normal	normal	complex	normal	normal
Drapebility	complex	complex	very simple	simple	simple
Producibility (dome + ring)	complex	complex	average	simple	simple
Conclusion	Second choice	Too heavy	Complex to make	Not applicable (strain)	Preference

* section close to ring/mid and/or top of hull

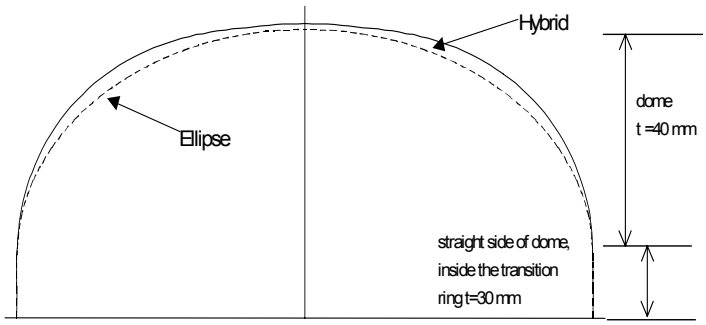

Fig. 3. Hybrid & ellipsoidal end-dome shape.

deployment and recovery. Various options, which incorporated many practical aspects and experience, were considered [6].

The choice of material for the transition rings was effectively only a choice between Aluminium or Titanium alloys. Aluminium, although cheaper and more readily available than Titanium, requires additional surface protection to prevent corrosion. Titanium offers higher strength and better corrosion resistance, but is more expensive and may be difficult to obtain in high strength grades for large diameter rings. An important point is the fact that CFRP has a potential of +0.1 V and is more noble than any other structural metal (Titanium –0.13 V, Steel –0.2 V, Aluminium –0.75 V), so care needs to be taken to ensure insulation of the CFRP from neighbouring metallic parts, even Titanium.

In the end two version of transition ring design were utilised, both of which use two rubber 'O'-rings, acting on different sealing faces, to form the seal. Simple rubber 'O'-rings have widely been proven to be most reliable, where dismantling and re-assembly is required. Although cleanliness is an essential prerequisite, large section 'O'-rings and the use of two seals allow greater tolerance to the working environment on board ships. One design incorporated a male and female V profile with 'O'-rings acting on each side face, with a bolted dovetail clamp arrangement. A schematic drawing of this design is shown in Fig. 4(a). This design was utilised in the long-term creep and hydrostatic test on the back-to-back domes, fabricated in Titanium Ti-6Al-4V (creep test) and Aluminium 6082-T6 (hydrostatic). The other design incorporated a face and corner seal, with a simpler bolting arrangement. This is simpler to machine and two sets were fabricated in Aluminium 6082-T6 for the large scale demonstrator test, Fig. 4(b).

4. TESTING AND COMPARISON WITH NUMERICAL RESULTS

4.1 Small scale cylinders

Axial compression and hydrostatic pressure tests were carried out on a series of small scale

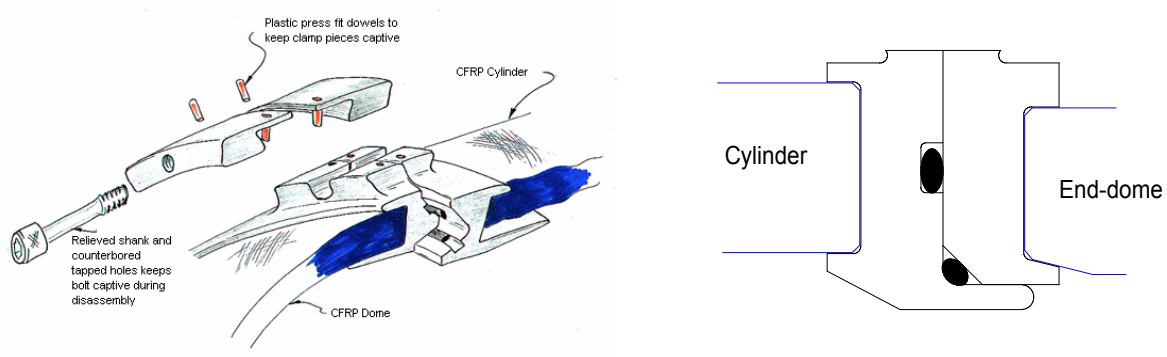

(a) (b)

Fig. 4. Schematic of vee profile (a) and of face and corner seal (b) transition ring.

CFRP cylinders of four different nominal wall thicknesses. Axial compression tests were conducted to condition the strain gauges installed around the circumference of the inner surface and to provide data from which the longitudinal Young's modulus, E_z, and the in-plane Poisson's ratio, $\nu_{z\theta}$, could be determined, based on a number of assumptions [7, 8].

The hydrostatic pressure tests were conducted within the ultra-high pressure chamber (UHPV, rated to 2,200 bar) at QinetiQ Rosyth. These tests provided data on the material's strength, the buckling and collapse pressures and failure modes for comparison with theoretical predictions and verification of the numerical or analytical codes. A typical strain record is shown in Fig. 5, with examples of a typical buckling failure mode in Fig. 6.

The thin, nominal 6 mm thick, cylinders were all very consistent both in terms of buckling (mode 3) and collapse pressure. The 8 mm thick cylinders, while reasonably consistent in terms of failure and buckling mode, all collapsed at lower pressures than the 6 mm cylinders, indicating that the problems observed in fabricating the thicker cylinders to the optimised winding sequence may have just started to become apparent. The detrimental effect of delamination and surface imperfection, fibre kink/waviness were clearly demonstrated. The good, 12 mm thick cylinder performed as expected, as did the 20 mm 'Case 4' cylinders which collapsed by material failure between 75 and 100 MPa.

The two small scale cylinders, fabricated with the same winding sequence as the large AUV demonstrator cylinder showed reasonable consistency, failing in mode 2 buckling with a collapse pressure between 60 and 71 MPa. This compares well with the optimised 'Case 4' cylinder which failed, again, in mode 2 buckling with a collapse pressure of 71.7 MPa. Typically buckling occurs at 95% of the final failure pressure, on the basis that the cylinder is defect free and that good consolidation has been achieved.

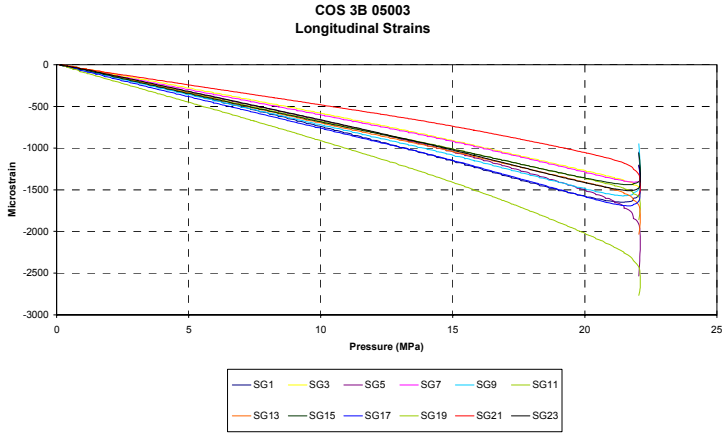

Fig. 5. Typical strain records during hydrostatic pressure testing.

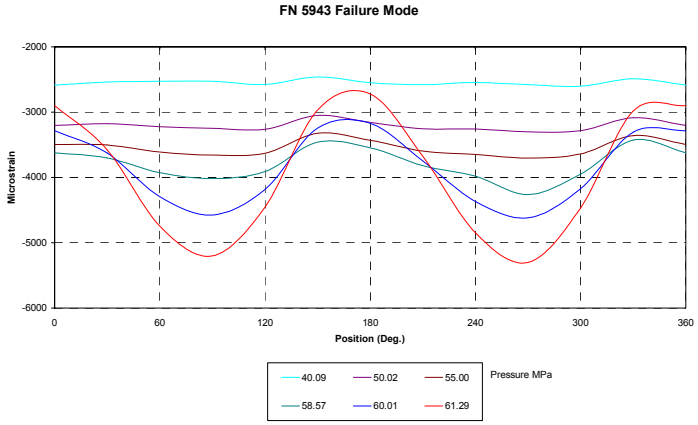

Fig. 6. Mode 2 buckling failure.

Table 4. Comparison of stacking sequence for large creep cylinder.

Thickness (mm)	$[90°_n/\pm55°_n]$ winding		$[\pm55°_n]$ winding	
	Eigenvalue buckling (MPa)	Non-linear (strain) analysis (MPa)	Eigenvalue buckling (MPa)	Non-linear (strain) analysis (MPa)
22	32.4	26.46	22.08	17.92
25	43.6	33.76	30.05	23.94
30	66.4	49.90	46.69	33.52
35	93.8	68.65	67.43	48.25
40	-	-	91.95	66.53

4.2 Long-term creep tests

A finite element parametric study [9] considered a full AUV hull, consisting of CFRP cylinder, Titanium transition rings and Titanium end-domes. In addition, it compared the $[90°_n/\pm55°_n]$ stacking sequence with a $[\pm55°_n]$ stacking sequence, which had been previously successfully used in a MAST-II AUV Project, Table 4. This study clearly indicated that for the desired working pressure of 20 MPa (2,000 metre sea depth) with a 1.5 factor of safety, a cylinder thickness of 24 mm was required for the $[90°_n/\pm55°_n]$ stacking sequence. This compares with a cylinder thickness in the order of 29 mm for the $[\pm55°_n]$ stacking sequence, a significant saving in terms of weight and manufacturing costs.

The cylinder was duly fabricated, strain gauged and instrumented with an internal battery powered data-logger, prior to installation within a benthic lander frame. In addition to the large creep cylinder, two sets of small scale cylinders (8 and 12 mm thick), strain gauged and with internal data-loggers, and one set of large CFRP end-domes in a back-to-back configuration were installed on the lander frame. The benthic lander was deployed from the NERC ship *Challenger* at the Porcupine Bite in 2,050 m of water during September 1999. It was recovered by the NERC ship *Discovery*, 373 days after deployment. On recovery it was obvious that three of the small scale cylinders had collapsed under pressure. The remains of two could be seen, with one completely missing. These were identified as being the 8 mm thick cylinders.

The failure of the 8 mm thick cylinders was, by this stage in the project, not totally unexpected. The poor performance of similar cylinders in the hydrostatic pressure tests had indicated a collapse pressure of only 18.6 MPa, approximately 200 m less than the deployment depth. A more serious and limiting knock-on effect of the collapse of these cylinders was the fact that only one of the remaining four data loggers was found to be fully operational when the cylinders (large and small) were dismantled.

Normalised and drift corrected data records from one small cylinder are shown in Fig. 7. At 2,000 m (approximately 20 MPa pressure) the cylinder had started to buckle in mode 2. The creep strain record indicates a general relaxation of the strains of between 270 and 407 μstrain over the duration of the creep tests (+0.03 ÷ +0.045 μstrain/hr).

Hydrostatic pressure tests were conducted on the three small cylinders recovered from the long-term creep test. This was done to establish if there were any lasting effects. The results indicated reasonable consistency with respect to buckling (Mode 2, at about 24 MPa) with a wider spread of collapse pressures, between 26.4 and 30.5 MPa.

Visual examination of the large creep cylinder and the back-to-back end-domes did not indicate any degradation of these test specimens. The CFRP cylinder, CFRP end-domes, transition rings and sealing mechanisms all performed satisfactorily in surviving both the close proximity shock loading when the three small cylinders collapsed and the 12 month deployment at 2,000 m.

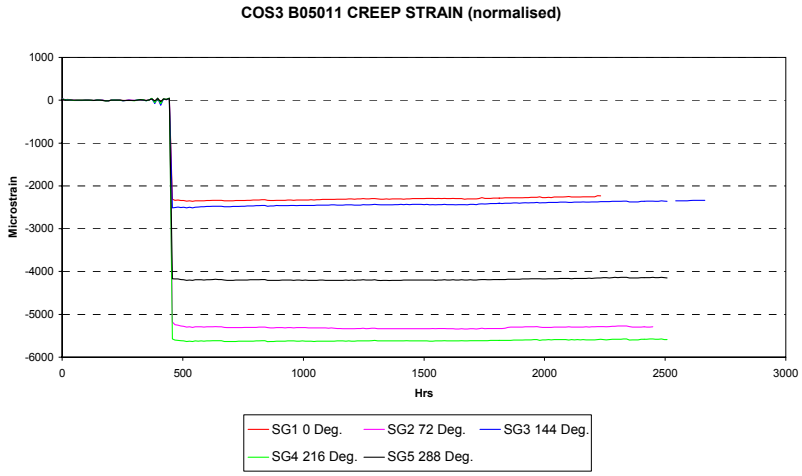

Fig. 7. Normalised creep strains.

4.3 End-dome test

A set of large RTM CFRP end-domes with Aluminium transition rings were subjected to hydrostatic pressure tests in a back-to-back configuration at within the 1000 bar ACB tank at IFREMER Brest [10]. The domes were instrumented with a total of 45 internal and 11 external strain gauges. A low level test to 5 bar conditioned the strain gauges and ensured that there were no leaks from either the transition rings or the central instrumentation connector/penetration in the apex of one of the domes. The test proceeded up to 542 bar (5,420 m) when the dome with the penetration collapsed. On dismantling it was found that the dome with the electrical connector/penetration had completely disintegrated. The other dome, although effectively still in one piece, had suffered major cracking and delamination.

4.4 AUV demonstrator test

Due to the reservations of potentially introducing delaminations within the cylinder if fabrication proceeded with the optimised winding sequence, it was decided to revert back to the second best winding sequence [90°n/(±θ)n] from the earlier work [2]. This allowed the completion of the numerical analysis and the specification of a cylinder wall thickness of 26.3 mm with a [90°n/(±55°)n], the 90°n layers being on the inside of the cylinder.

The cylinder was fabricated, by CNIM [4], to an oversized thickness of 28 mm (as a result of further analysis), the first 8 mm with a 90° (hoop) winding followed by intermediate curing, then two 10 mm covers with ±55° (nominal) winding with intermediate and subsequent final curing. The quality of fabrication was checked by an ultrasonic inspection, which gave no indications of any flaws, delamination or porosity. Finally, the cylinder was machined and the transition rings bonded to the ends.

Prior to testing, a total of 117 strain gauges were applied to the internal surfaces of the demonstrator, comprising 25 gauges on the aft end-dome, 72 gauges on the cylindrical body and 20 gauges on the forward end-dome, which includes a penetration for the instrumentation connectors. The pressure test was carried out at IFREMER Brest [11]. As in the back-to-back end-dome test, a low level test to 5 bar conditioned the strain gauges and ensured that there were no leaks from either the transition rings or the central instrumentation connectors/penetration in the apex of the forward dome. The final collapse pressure attained was 398 bar (3,980 m) by failure of the cylinder in mode 2 buckling. The strain gauge records from both end-domes indicated a linear response up to 350 – 360 bar, the highest strain being in the order of -7,000 μstrain. The records from the cylinder indicated a linear response up to 350 bar, whereas at 360 bar mode 2 buckling was established.

4.5 Comparison of test and numerical results

Tables 5 and 6 provide comparison of the test results with the various finite element analyses conducted. Details of each analysis can be found in the references cited for each case.

Table 5. Predicted loads for small scale cylinders (MPa).

Thickness (nom)	6 mm	8 mm	12 mm	12 mm	20 mm
Winding sequence	Case 4	Case 4	Mod. Case 4	Demonstrator	Case 4
Ave. test pressure, MPa (buckling)	20.95	16.03	68.56	63.29	-
Ave. test pressure, MPa (collapse)	21.96	18.60	71.69	66.09	88.50
Eigenvalue buckling [12]	27.1	45.7	102.0	88.8	-
Non-linear buckling [12]	23.6	39.6	85.6	76.6	-
Strain [12]	20.5	-	74.0	61.0	-
Material failure [12]	22.3	31.5	44.3	-	-
Eigenvalue buckling [13]	19.3	38.5	98.2	-	227.2
Material failure [13]	27.4	32.3	58.4	-	103.0

Table 6. Predicted buckling of demonstrator.

	NTUA		**IFREMER**		**QinetiQ**	**Experimental**
	Eigenvalue	**Non-linear**	**Eigenvalue**	**Non-linear**	**Non-linear**	
4-node shell elements	44.5 MPa	34.7 MPa	-	-	38.6 MPa	
8-node solid elements	36.5 MPa	31.6 MPa	33.2 MPa	≈28.0 MPa	-	39.8 MPa
Mode shape	Mode 2	Mode 2	Mode 2	Mode 2	Mode 2	Mode 2

5. CONCLUSIONS

Theoretically, the optimised stacking sequence results in a stiffer cylinder, with typically a minimum 11.5% increase in buckling load. However, there are problems in production with a complex winding sequence, poor consolidation and delaminations, particularly with lower winding angles. The best compromise was found to be a multi-step winding and curing manufacturing process, which was successfully applied to the large AUV demonstrator cylinder with a $[90°_n/(\pm 55°)_n]$ stacking sequence. The detrimental effect of delamination and surface imperfections was clearly demonstrated in the results of the small scale cylinder tests.

Overall the long-term material test was of limited success. The method of deployment and recovery of the benthic lander were successful, as was the design and fabrication of the large RTM composite end-domes and large filament wound composite creep cylinder. The loss of three small cylinders severely limited the amount of data obtained, not only by the loss of these cylinders but also by the loss of two more data loggers due to the resulting close proximity shock loading when these cylinders collapsed.

The design (ellipsoidal shape), fabrication (RTM), stress analysis and subsequent destructive testing of the large composite end-domes more than met the desired working depth of 2,000 m with a factor of safety of 1.5. A collapse pressure of 54.2 MPa was attained with virtually linear response up until failure, suggesting that a slightly thinner end-dome configuration would be practical with the resulting weight saving.

The successful design, analysis and fabrication of a large scale, all composite, AUV pressure

hull, as demonstrated by the subsequent pressure test, was fundamental to the objectives of the project. The design exceed the required 30 MPa target (2,000 m operational depth with a 1.5 factor of safety) with buckling occurring at about 35 – 36 MPa with collapse at 39.8 MPa. The numerical analysis tools indicated that acceptable predictions can be made if attention is given to the mechanical properties, the mesh refinement and choice of finite elements, and the geometrically non linear behaviour of the hull.
All of the above points, along with a specification checklist, guidelines on material selection and production techniques, and a relative cost comparison, have been incorporated within a single document [14].

ACKNOWLEDGEMENTS

The authors would like to acknowledge the financial support of the European Commission through contract no MAS3-CT97-0091: *Lightweight composite pressure housings for mid-water and benthic applications*, which partially financed the research that led to the results presented in this paper.

References

1. **Olijslager, J.** and **Antonelli, V.**, *Lightweight composite pressure housings for mid-water and benthic applications – Task 1: Requirements and material selection*, CLC TUD-TNO report no. CLC 283-98040ljor, April 1999.
2. **Papazoglou, V.J., Tsouvalis, N.G.** and **Zaphiratou, A.**, *Parametric study of small scale composite cylinders under hydrostatic load: Flat rigid end-closures*, NTUA report no. STL-073-F-98 Rev. 1, November 1998.
3. **Rosborough, I.W.C., Campsie, G.P.** and **Livingstone, F.**, *Composite cylinder flat plate end-closures, Design optimisation*, DERA report no. DERA/MSS7/TR980455, September 1998.
4. **Jennequin, G.** and **Micheaux, D.**, *Fabrication report*, CNIM report no. COS3B0300 /52 J001, March 2002.
5. **Antonelli, V.** and **van Tooren, M.**, *Design of composite pressure hull end-closures*, SAMPE Europe, March 2001. Centre of Lightweight Structures TUD-TNO report, *Conceptual design of end-domes*, Report no. TNO CLC 283-980801vvtr, September 1998.
6. **Stevenson, P.** and **Nederveen, P.J.**, *Report on transition ring sealing and fixing designs*, MAS3-CT97-0091 Task 1: Requirements and Material Selection, November 1998.
7. **Livingstone, F.**, Task 4.1: *Tests of 175mm internal diameter cylinders with flat plate end closures*, DERA report no. DERA/MSS/MSTR1/TR010972, January 2001 (Draft).
8. **Chauchot, P., Le Flour, D., Livingstone, F.** and **Warnier, P.**, *Task 4: Testing – Final report*, IFREMER report no. R.INT.TMSI/RED/MS-01-129, January 2001.
9. **Zaphiratou, A., Tsouvalis, N.G.** and **Papazoglou, V.J.**, Numerical study of large creep cylinder under hydrostatic load, NTUA report no. STL-076-F-98 Rev.1, July 1999.
10. **Warnier, P.**, *Task 4.4: Hydrostatic test on demonstrator composite dome end closures*, IFREMER report no. TMSI/RED/EM 00.191, January 2001.
11. **Warnier, P.**, *Task 4.6: Hydrostatic test on demonstrator*, IFREMER report no. TMSI/RED/EM 01.137, January 2001.
12. **Zaphiratou, A., Tsouvalis, N.G.** and **Papazoglou, V.J.**, *Task 2.3: Comparison of numerical and/or theoretical results with experiment*, NTUA report no. STL-092-F-00, December 2000.
13. **Graham, D.**, Analysis of small scale cylinders with flat end closures, DERA report no. DERA/MSS/MSTR1/TR000107, January 2000.
14. **van Tooren, M., Tsouvalis, N.G., Antonelli, V., Livingstone, F., Jennequin, G., Bigourdan, B.** and **Graham, D.** , *Design tools for AUV's*, MAS3-CT97-0091 Task 5: *Proposed design and fabrication procedures*, TNO report no. 340-991222-2VAR, March 2001.